Energy 215 (2021) 118956

Contents lists available at ScienceDirect

Energy

journal homepage: www.elsevier.com/locate/energy

System impact of heat exchanger pressure loss in ORCs for smelter off-gas waste heat recovery

Monika Nikolaisen [a, *], Trond Andresen [a]

[a] SINTEF Energy Research, Department of Gas Technology, Sem Sælands Vei 11, 7034, Trondheim, Norway

ARTICLE INFO

Article history:
Received 9 February 2020
Received in revised form
10 September 2020
Accepted 27 September 2020
Available online 6 October 2020

Keywords:
Waste heat recovery
Aluminum smelter off-gas
ORC optimization
Heat exchanger pressure loss
Hydrocarbon working fluid

ABSTRACT

Applying Rankine cycles to smelter off-gas could increase the required off-gas fan power in an order of magnitude equivalent to the power production. Predicting the fan power is not straightforward since it is affected in two contradictory ways: 1) the heat recovery heat exchanger creates additional off-gas pressure loss, increasing fan power; 2) off-gas cooling reduces pressure loss in the off-gas handling system downstream of the cycle, reducing fan power. The purpose of our study is to analyze the effect of fan power on optimum system performance. While additional fan power can be calculated based on heat exchanger pressure loss, the reduction in fan power depends on the total pressure loss downstream of the cycle, which is unknown. As an alternative to calculating fan power reduction, we account for the off-gas cooling effect by including only parts of the fan power caused by heat exchanger pressure loss. Results from three cases show that both heat exchanger and cycle performance strongly depend on the potential for downstream pressure loss reduction. Thus, the total pressure loss in the downstream off-gas handling system has a significant impact on the optimum heat exchanger and cycle performance, and should be accounted for during system design.

1. Introduction

The aluminum industry is one of the most energy intensive industries in the world [1], and accounts for around 3.5% of global electricity consumption and 1% of global CO_2 emissions [2,3]. In Norway, aluminum production represents about 17% of all inland electricity consumption [4]. Still, the aluminum industry is expected to consume even more energy in the future, as the demand for aluminum is projected to increase 2–3 times by 2050 [2]. The industry has targeted a 50% reduction in emissions by 2050, meaning that, in practice, the specific emissions have to be reduced by at least 75% [2].

Around half of the energy input to aluminum smelters is lost to the surroundings as surplus heat [5–7]. Recovering this surplus heat could significantly improve energy efficiency and reduce emissions in the aluminum industry. The two most efficient ways of utilizing surplus heat are direct re-use at the same temperature level and upgrading to a higher temperature level using a heat pump. However, such reutilization is limited in the aluminum industry owing to the low quality of rejected heat and a lack of nearby demand for heat [5]. Further research is necessary to pave the way for cost-efficient and large-scale surplus heat utilization in the aluminum industry.

An option for more widespread utilization of surplus heat in the aluminum industry is conversion into electric power, or "heat-to-power" conversion. Heat-to-power conversion can be realized using Rankine cycles, also known as organic Rankine cycles (ORCs) when utilizing an organic working fluid. Research on Rankine cycles covers a broad range of application areas and research topics. A few examples include power production from engine waste heat [8,9], geothermal heat [10,11] and solar heat [12], and evaluation of expander technology [13–15], cycle architecture [16,17], and thermo-economic analysis [10,18,19]. Our article focuses on the particular challenges concerning application of Rankine cycles for surplus heat-to-power conversion in the aluminum industry. However, results could also be valid for other industries with similar heat source characteristics and boundary conditions.

There are several potential surplus heat sources that can be recovered at primary aluminium production facilities. Our study focuses on surplus heat originating from the electrolytic reduction process. This process takes place in a series of aluminum electrolysis cells, as illustrated in Fig. 1. In this example, the electrolysis

* Corresponding author.
E-mail addresses: monika.nikolaisen@sintef.no (M. Nikolaisen), trond.andresen@sintef.no (T. Andresen).

https://doi.org/10.1016/j.energy.2020.118956

Nomenclature

A	heat transfer surface area (m^2)
A_c	cross-sectional flow area (m^2)
d_h	hydraulic diameter (m)
h	enthalpy (kJ/kg)
HRHE	heat recovery heat exchanger (−)
L	length (m)
$\dot{m}$	mass flow (kg/s)
η	efficiency (−)
p	pressure (Pa)
P	perimeter (m)
$\dot{Q}$	heat duty (kW)
s	entropy (kJ/kgK)
U	overall heat transfer coefficient (W/m^2K)
$\dot{W}$	power (kW)
Δp	pressure loss (Pa)
ΔT_{min}	pinch point temperature difference (K)
$\Delta \dot{W}$	change in power (kW)

Subscript

cond	condenser
evap	evaporator
exp	expander
gas	electrolysis cell off-gas
gen	generator
ind	indirect fluid
is	isentropic
mech	mechanical
rec	recuperator
sink	heat sink
source	heat source
tot	total
wf	working fluid

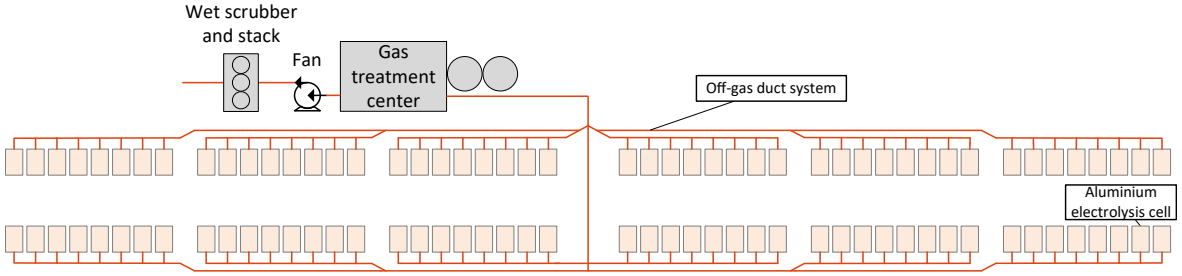

Fig. 1. Sketch of a generic primary aluminum production facility.

cells are organized in clusters of eight, and a duct system transports the off-gas from the cells to a gas treatment center, fan, wet scrubber and stack. The fan recovers the total off-gas pressure loss through the system. Surplus heat from the electrolysis cells mainly takes the form of heat dissipation through the steel shell of the electrolysis cells, and as heat contained in the warm off-gas exiting the cells.

Utilization of surplus heat dispersed through the sidewalls of aluminum electrolysis cells has been investigated in several research articles [1,20,21]. This heat source has a relatively high exergy content, i.e. potential for power production, owing to the temperature level of the rejected heat, which typically ranges between 200 and 350 °C [1,22]. However, recovering heat from the electrolysis sidewalls is challenging because it can affect the thermal energy balance of the electrolysis process itself, the sidewalls are difficult to access and the smelter environment is chemically reactive [1]. Moreover, utilizing the heat rejected through the sidewalls would require new infrastructure in connection to a large number of electrolysis cells, as evident from Fig. 1.

Recovering the heat contained in the electrolysis off-gas is an interesting alternative to utilization of heat rejected from the sidewalls. The off-gas mainly consists of air infiltrated into the cells and CO_2 released in the electrolytic reduction process [5]. Air infiltration is necessary for operational reasons and to limit fluoride emissions, and significantly reduces the temperature of the off-gas [23]. The off-gas typically exits the cells at a temperature in the range 150–180 °C, depending on ambient temperature and other factors [24–26]. Since the off-gas has a relatively low temperature, the specific potential for power production is limited. However, the total energy content in the gas could be significant and in some cases larger than that dispersed through the sidewalls [22]. Utilization of the off-gas also has several practical advantages. First of all, the off-gas is considered the most easily accessible heat source at aluminum facilities since it is already collected in ducts and chimneys [7,22]. Moreover, off-gas utilization requires no or only minimal structural modifications to the electrolysis cells, and does not have a significant influence on the thermal energy balance of the cells [27,28]. We focus on off-gas surplus heat utilization due to its practical advantages and significant energy content. However, other heat sources at aluminum plants are also important to investigate to maximize surplus heat recovery.

Conversion of surplus heat to power is challenging in general because of low cost-efficiencies [1]. Surplus heat sources with low specific energy density,[1] such as aluminum smelter off-gas, introduce additional challenges; the heat recovery heat exchanger will create additional off-gas pressure loss and thereby contribute to additional fan power consumption. Due to the large volume flow of the gas, the additional fan power could be significant compared to the power production, and in some cases equal in magnitude to the power output [7]. Thus, accounting for fan power during power cycle optimization is critical to system performance. As can be seen in the following, previous research has been insufficient in accounting for the off-gas fan power during Rankine cycle optimization. Even when the change in fan power has been calculated, the

[1] Aluminum electrolysis off-gas is similar to air in thermodynamic properties at approximately atmospheric pressure and a temperature in the range of 150–180 °C.

analyses are limited by fixed heat recovery heat exchanger parameters. Note that auxiliary power on the heat sink side could also be of a significant magnitude, especially in the case of air cooling. However, our study involves a water heat sink with a relatively small ratio of pumping power to net power.

Research on off-gas heat-to-power conversion has covered different topics, such as optimization of Rankine cycle working fluid and operating conditions [29,30]. The effect of an off-gas cooling limit has also been investigated, which is necessary to avoid corrosion problems caused by condensation of acidic components [31]. Ladam et al. [31] investigated the effect of such a cooling limit on Rankine cycles that recover heat from the source both directly and indirectly through an indirect heat transfer loop. Their results showed that the cooling limit had less impact on indirect cycles than direct cycles, but the latter achieved higher power output. Other studies have analyzed the potential for implementation of Rankine cycles at existing aluminum plants in the Nordic countries. For instance, Yu et al. [7] investigated both Rankine cycles and combined heat and power cycles at Alcoa's plant in Fjardaal, Iceland. They found that the Rankine cycles achieved the highest exergy efficiency, whereas the combined heat and power cycles achieved the highest energy efficiency. Another example is Børgund [32], who evaluated implementation of Rankine cycles at Hydro's plant in Øvre Årdal, Norway. One of her findings was that Rankine cycles were more suitable than other power cycles, such as Stirling engines, steam cycles and Kalina cycles. A similar conclusion was reached by Kolasiński [33], who concluded that the Rankine cycle was a promising technology for heat-to-power conversion in the metal smelting industry.

The design of heat exchangers for off-gas heat recovery is also an important research topic, since such heat exchangers are prone to fouling and abrasion [34]. Fouling of heavy dust particles is critical to performance and should be avoided, as it reduces heat transfer coefficient, increases pressure drop and requires expensive maintenance [28]. We have assumed that fouling does not affect the performance of the heat recovery heat exchanger based on the assumption that fouling can be avoided using circular channels without surface enhancements [24,35].

Our scope is to investigate the effect of off-gas fan power on optimum system performance, which is not a trivial task. As mentioned, fan power increases due to off-gas pressure loss in the heat recovery heat exchanger. At the same time, off-gas cooling contributes to a *reduction* in fan power, due to reduced volume flow in the downstream gas collection and treatment system [7,32]. The magnitude of the fan power reduction is not only dependent on the reduction in off-gas temperature and volume flow, but also on the total pressure loss in the downstream gas collection and treatment system, since fan power is proportional to both volume flow and pressure loss. Another important effect is that power production can increase with higher off-gas pressure loss through the heat recovery heat exchanger, due to the positive correlation between heat exchanger pressure loss and heat transfer coefficient [36].

Some research articles have calculated the change in fan power when implementing a Rankine cycle for heat-to-power conversion from aluminum smelter off-gas. For example, Børgund [32] found that Rankine cycle implementation resulted in a net *decrease* in fan power compared to the baseline scenario. However, the cycle she evaluated was not optimized, but rather simulated based on a number of fixed parameters, such as an off-gas heat exchanger pressure loss of 1000 Pa and a pinch point temperature difference of 15 °C in the heat recovery heat exchanger. Børgund stressed that the calculated effect on fan power should only be seen as a preliminary indication due to the simplifications made. Furthermore, the analysis is only valid for the specific evaluated aluminum plant, with a nominal pressure difference of about 5000 Pa across the off-gas fan. Thus, the results cannot be generalized to plants with different pressure loss in the gas collection and treatment system.

Yu et al. [7] accounted for the change in off-gas fan power during Rankine cycle optimization. They formulated an equation for net power that included the additional fan power due to off-gas heat exchanger pressure loss, as well as the reduction in fan power due to off-gas cooling. They optimized the Rankine cycle using a multi-objective optimization approach with the purpose of finding an optimal compromise between net power, exergy efficiency and heat transfer surface area. The resulting net power was 1.2 MW, accounting for 2.4 MW additional fan power due to off-gas heat exchanger pressure loss, and 1.3 MW reduction in fan power due to off-gas cooling. Although the study accounted for the change in fan power during optimization, the analysis involved several simplifications, such as fixed heat exchanger geometries (i.e. no heat exchanger geometry optimization) and a fixed off-gas pressure loss and heat transfer coefficient. Thus, the optimization tool had limited freedom to optimize performance, and there may be a higher net power with a more optimal compromise between power production and fan power. Furthermore, the results are only valid for the specific evaluated aluminum production facility. In any case, it is worth noting that the net increase in fan power, 1.1 MW, was approximately the same as the net power, demonstrating the importance of accounting for fan power during cycle optimization.

While a few studies have accounted for the change in off-gas fan power in Rankine cycle analysis, the performance of the heat recovery heat exchanger has not been optimized. Furthermore, no in-depth analysis has been made of how fan power affects system performance under different boundary conditions. To close this research gap, our study evaluates the effect of fan power on optimum system performance by optimizing both heat exchangers and cycle operating conditions simultaneously. We do not evaluate a specific nominal pressure loss in the downstream gas collection and treatment system. Instead, we evaluate different downstream conditions, and thus different potential for fan power reduction, by including only parts of the fan power caused by heat exchanger pressure loss. The underlying assumption is that the part of fan power from heat exchanger pressure loss that is not included can be compensated for by an equivalent reduction in fan power from off-gas cooling. We analyze the two extreme cases, which include none and all of the fan power from heat exchanger pressure loss, respectively. The optimal solution will lie somewhere between these two extremities, depending on conditions in the downstream off-gas handling system. In addition to the two extreme cases, we analyze a case that includes half of the fan power from heat exchanger pressure loss, representing a more practical solution.

The analysis may contribute to improving the energy recovery potential in the smelting industry by enabling a better understanding of how Rankine cycles and heat exchangers should be designed for optimum performance.

2. Methods

2.1. Case description

Fig. 2 shows a sketch of a generic aluminum production facility in a scenario with heat-to-power conversion from the electrolysis off-gas. Several Rankine cycles are placed throughout the plant to recover surplus heat close to the cells at a high off-gas temperature. For simplicity, the system boundary of the analysis only encompasses one Rankine cycle, recovering surplus heat from a cluster of eight electrolysis cells. Due to the methodology used, considering more or all the Rankine cycles would have no effect on optimization results.

The off-gas exits the cells at a temperature of 150 °C and is

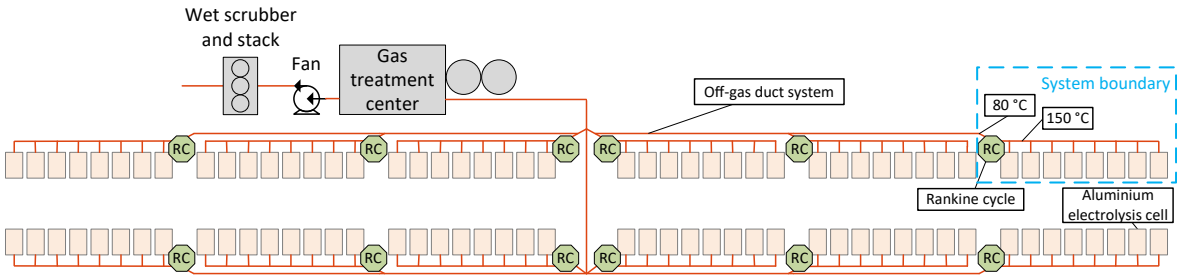

Fig. 2. Sketch of a generic primary aluminum production facility with heat-to-power conversion from off-gas.

collected in a duct system that transports the off-gas to the gas treatment center, fan, wet scrubber and stack. The fan recovers the total off-gas pressure loss through the system. When there is no surplus heat recovery, we refer to this pressure loss as the nominal pressure loss. Implementing a Rankine cycle will affect the nominal pressure loss and thereby the fan power in two ways: 1) additional pressure loss through the heat recovery heat exchanger, increasing fan power, and 2) reduction in pressure loss due to off-gas cooling, reducing fan power. Both effects are accounted for in our study.

Table 1 and Table 2 show the heat source and heat sink specifications, respectively. The off-gas heat source is modelled as air, which is assumed to provide sufficient thermodynamic accuracy. We have imposed a lower cooling limit of 80 °C on the off gas to avoid condensation of acidic components. The acid dew point depends on many factors and is difficult to determine, and 80 °C represents a typical conservative limit [37,38]. The heat sink is cooling water at 10 °C, which is a representative annual mean temperature in the Nordic countries. The heat sink mass flow was set to 23 kg/s, which was the optimal value resulting from preliminary system optimizations, as described in Section 3 Results and discussion.

Table 2
Heat sink specifications.

Heat sink	Unit	Value
Fluid	–	Water
Inlet temperature	(°C)	10
Mass flow	(kg/s)	23
Pressure	(bar)	5.0

2.2. Rankine cycle model

The modelled Rankine cycle is sketched in Fig. 3. Heat is recovered indirectly from the heat source through a heat recovery heat exchanger (HRHE). A heat source fan is located downstream of the HRHE to calculate the additional fan power caused by off-gas heat exchanger pressure loss. The indirect heat transfer loop uses pressurized water as heat transfer fluid, which is commonly used in industrial applications of aluminum off-gas energy recovery [23,26]. An indirect system solution was chosen since the working fluid is a flammable hydrocarbon, which receives heat from the indirect fluid through the evaporator and produces power in a Rankine cycle. Excess heat is transferred to the heat sink in the condenser. The model is generic with respect to subcritical and transcritical operation, which for all simulations in this work is determined by the solver manipulating the variable *expander inlet pressure*.

The cycle model has been developed based on the model described by Hagen et al. [36]. In our work, their model has been adapted from a direct cycle to an indirect cycle, and a heat source fan has been added. The heat exchangers modelled by Hagen et al. [36] were only geometrically described on the working fluid sides, with the exception of the recuperator, which was described on both sides. In our model, all heat exchangers are geometrically described on both sides. The modifications to the model and assumptions made by Hagen et al. [36] are summarized in Table 3. REPROP 9 was used for calculating thermodynamic properties [39] in both models.

The cycle model contains several heat exchangers, as well as pumps, an expander, and a heat source fan. The heat exchanger model is described in Section 2.2 Heat exchanger model. The models for the expander, pumps, and fan require the inlet state and

Table 1
Heat source specifications.

Heat source	Unit	Value
Fluid	–	Air
Inlet temperature	(°C)	150
Lower cooling limit	(°C)	80
Mass flow	(kg/s)	12
Pressure	(bar)	1.0

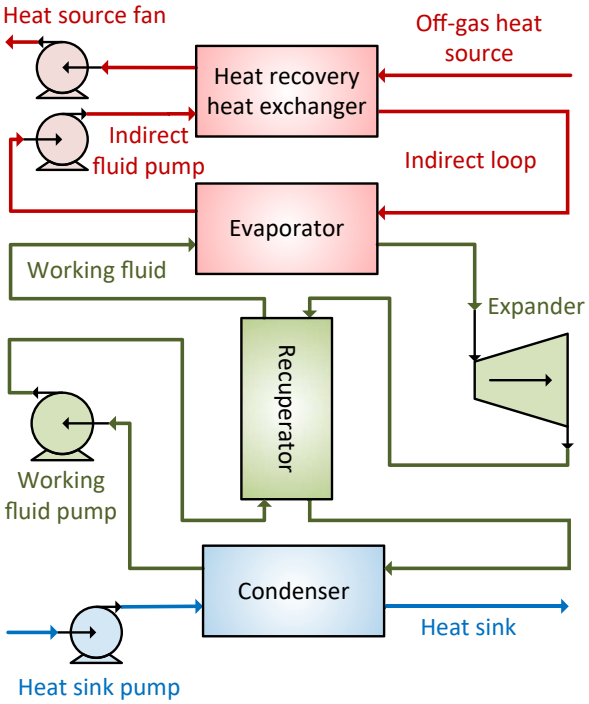

Fig. 3. Sketch of the modelled Rankine cycle.

Table 3
Modifications to the method used by Hagen et al. [36].

	Hagen et al. [36]	Our method
Heat source	Pressurized water at 140 °C.	Electrolysis off-gas at 150 °C.
Process	Direct Rankine cycle without heat source auxiliary equipment.	Indirect Rankine cycle with heat source fan, pressurized water as heat transfer fluid.
Heat exchangers	Geometries described on working fluid sides only. Working fluid side surface area used in calculations of heat exchanger area.	Geometries described on both hot and cold sides. Hot and cold side average surface area used in calculations of heat exchanger area.
Working fluid	Propane, propene, n-butane, mixture between propene and n-butane, R-134a.	Propene.

outlet pressure to be specified and are modelled with constant isentropic and mechanical efficiencies according to Eq. (1) through (4). From the saturated liquid state at the condenser outlet, the components are calculated in sequence, and fluid states are updated along the way. Two equality constraints are imposed to ensure that the pressure and temperature on each side of a stream split point are identical. Two inequality constraints requiring dry vapour at expander inlet and outlet are also included. Optimization variables, the objective function and additional constraints are described in Table 6.

Pump and fan model:

$$\eta_{is} = \frac{h(p_{out}, s_{in}) - h_{in}}{h_{out} - h_{in}} \tag{1}$$

$$\dot{W}_{pump} = (1 / \eta_{mech})\dot{m}(h_{out} - h_{in}) \tag{2}$$

Expander model:

$$\eta_{is} = \frac{h_{in} - h_{out}}{h_{in} - h(p_{out}, s_{in})} \tag{3}$$

$$\dot{W}_{exp} = \eta_{gen}\dot{m}(h_{in} - h_{out}) \tag{4}$$

Hagen et al. [36] compared the performance of five different hydrocarbon working fluids. They allowed the optimization solver to choose between subcritical and transcritical process design for each fluid, and found that four of the five investigated fluids resulted in transcritical configuration under optimal conditions. The only fluid that resulted in subcritical configuration under optimal conditions was n-butane, which achieved lower power output than the other fluids for the same values of total heat transfer area. The poor performance of the subcritical fluid owed in part to relatively low heat transfer coefficients. Based on the results from Hagen et al. [36] and the similar conditions in our work, we have chosen propene as the working fluid in this study.

The Rankine cycle net power is given by Eq. (5):

$$\dot{W}_{net} = \dot{W}_{exp} - \dot{W}_{wf\ pump} - \dot{W}_{sink\ pump} - \dot{W}_{ind\ pump} - \Delta\dot{W}_{fan,net} \tag{5}$$

$\Delta\dot{W}_{fan,net}$ refers to the net change in fan power caused by implementing a Rankine cycle, which is given by $\Delta\dot{W}_{fan,net} = \Delta\dot{W}_{fan,HRHE} - \Delta\dot{W}_{fan,cooling}$. The value of $\Delta\dot{W}_{fan,HRHE}$ is the additional fan power caused by heat exchanger pressure loss, and the value of $\Delta\dot{W}_{fan,cooling}$ is the reduction in fan power caused by off-gas cooling. Table 4 gives an overview of the two effects on fan power.

While the value of $\Delta\dot{W}_{fan,HRHE}$ can be calculated based on off-gas heat exchanger pressure loss, the value of $\Delta\dot{W}_{fan,cooling}$ depends on unknown factors outside the system boundary. To evaluate different boundary conditions, we investigate three cases that include different parts of the fan power caused by heat exchanger pressure loss:

Case 1. :

- Fan power is not included in the calculation of net power, i.e. $\Delta\dot{W}_{fan,net} = 0$
- For this to hold, the fan power reduction from off-gas cooling would have to equal the fan power from heat exchanger pressure loss

Case 2. :

- Half of the fan power from heat exchanger pressure loss is included in the calculation of net power. i.e. $\Delta\dot{W}_{fan,net} = 0.5 \cdot \Delta\dot{W}_{fan,HRHE}$
- This case could represent a scenario where fan power reduction equals half the fan power from heat exchanger pressure loss

Case 3. :

- The total fan power from heat exchanger pressure loss is included in the calculation of net power, i.e. $\Delta\dot{W}_{fan,net} = \Delta\dot{W}_{fan,HRHE}$
- This case disregards the reduction in fan power, and as such represents the strictest boundary conditions

Table 4
Description of the two different effects on fan power.

Effect on fan power	Description	Value
$\Delta\dot{W}_{fan,HRHE}$	Additional fan power caused by off-gas pressure loss in the heat recovery heat exchanger	Known Function of pressure loss in heat recovery heat exchanger
$\Delta\dot{W}_{fan,cooling}$	Reduction in fan power caused by off-gas cooling and reduced pressure loss outside the system boundary	Unknown Function of pressure loss outside system boundary

2.3. Heat exchanger model

The heat exchanger model is based on the generic heat exchanger model described by Hagen et al. [36], which is a simplified heat exchanger model that is able to account for heat transfer mechanisms and calculate heat transfer area without specifying the heat exchanger type. The model simply assumes that

Table 5
Heat transfer and pressure drop correlations.

Flow	Heat transfer	Pressure loss
Single-phase	Gnielinski [40]	Selander [41]
Two-phase	Boyko and Kruzhilin [42] (condensation)	Friedel [43] with single-phase formulation by Selander [41]

the hot and cold side fluids flow counter-currently through channels, and only specifies the hydraulic channel diameters, cross-sectional flow areas and channel length, e.g. d_h, A_c and L. The hydraulic diameters and flow areas differ on the hot and cold sides, whereas the channel length is the same. The heat transfer area on each side of the heat exchanger is given by $A_{cold/hot} = P_{hot/cold} \cdot L$, where P refers to the perimeter, given by $P = (4 \cdot A_c)/d_h$.

Based on these geometry parameters and fluid state points in one end of the heat exchanger, the heat exchanger model calculates heat duty, overall heat transfer coefficient, pressure loss and heat transfer area. The calculations are performed by solving three differential equations in a set of equidistant numerical integration steps, as described by Hagen et al. [36]. Local fluid properties, heat transfer coefficients and pressure gradients are evaluated for each integration step.

In the absence of in-depth economic functions per component, the sum of all heat exchanger areas could be considered as an initial representation of system costs. At initial design stages, it is not obvious whether the hot or cold side of the heat exchangers has the highest cost, and therefore the average area is used in the calculation of total area, i.e. $A_{HX} = (A_{cold} + A_{hot})/2$. The total heat transfer surface area in the Rankine cycle is given by $A_{tot} = A_{HRHE} + A_{evap} + A_{cond} + A_{rec}$.

Heat transfer and pressure loss correlations are given in Table 5, and are the same as those applied by Hagen et al. [36]. As Hagen et al. [36] pointed out, these correlations could be considered suitable to apply in the generic heat exchanger model, even for fluids not considered during development of the correlations. Note that we have not reported a correlation for boiling since all optimizations resulted in transcritical operation.

2.4. System optimization

An overall system optimization was performed for each of the three cases, which involves maximizing net power by optimizing cycle operating conditions and heat exchanger geometries simultaneously. The system is optimized using the gradient-based constrained optimization solver NLPQL [44]. The objective function, optimization variables and constraints are given in Table 6. Based on the value of optimized variables and boundary conditions, all operating conditions in the system can be calculated. Note that expander inlet pressure is a free optimization variable, which means that the solver can choose between subcritical and transcritical process designs.

Each case was subjected to the same constraint on a total heat transfer surface area of 750 m^2 to ensure a fair comparison between the different cases. Note that this means the heat exchangers were not constrained by a minimum pinch point temperature difference. With a constraint on total surface area, the solver will search for the heat exchanger geometry parameters that yield the optimal heat transfer area distribution between the four heat exchangers, as well as the optimal trade-offs between overall heat transfer coefficients and pressure losses. A heat transfer area of 750 m^2 was set in this particular case to represent a relatively large system with small temperature differences, utilizing most of the available potential in the heat source. Furthermore, the maximum off-gas heat exchanger pressure loss was set to 5000 Pa to avoid unlimited pressure loss in Case 1, where fan power is not included in the objective function. Observe that heat exchanger length is an optimization variable, meaning that the optimizer can choose a recuperator length of 0 if this is optimal. Thus, a recuperator is only included if it results in a higher net power.

Fixed parameters are given in Table 7. A number of parameters were fixed to simplify the optimization problem, including the cross-sectional flow area on the heat sink side of the condenser, fixed to 100 cm^2, and the working fluid outlet pressure at the condenser outlet, fixed to 10 bar. Heat exchanger hydraulic diameters were also fixed during optimization. It was assumed that sufficient heat exchanger optimization flexibility is achieved by optimizing heat exchanger length and cross-sectional flow areas. This assumption is evaluated in Section 3 Results and discussion.

3. Results and discussion

Table 8 shows the main results from system optimization. Note that an overall system optimization was performed for each of the cases. Observe first Case 1, where fan power was not included during optimization, i.e. $\Delta \dot{W}_{fan,net} = 0$. For this reason, the optimizer makes no effort to minimize off-gas pressure loss, which reaches the upper limit of 5000 Pa. As a result, fan power from off-gas heat exchanger pressure loss becomes relatively high, amounting to almost half of the power produced in the expander. This is likely an unfeasible solution, demonstrating the need for including fan power during optimization, or alternatively to set a more practical upper limit on maximum off-gas pressure loss. However, it is unlikely that setting such a limit results in the most

Table 6
Objective function, optimization variables and constraints.

	Symbol	Description
Objective function	$\dot{W}_{net}$	Net power
Process optimization variables	$\dot{m}_{wf}$	Working fluid mass flow
	$\dot{m}_{ind}$	Indirect fluid mass flow
	$h_{in,exp}$	Expander inlet enthalpy
	$p_{in,exp}$	Expander inlet pressure
	$T_{out,HRHE,ind}$	Indirect fluid outlet temperature from the HRHE
Heat exchanger optimization variables	L	Channel length
	$A_{c,hot}$	Hot side cross-sectional flow area
	$A_{c,cold}$	Cold side cross-sectional flow area
Constraints	A_{tot}	Total heat transfer surface area
	$\Delta p_{HRHE,max}$	Max HRHE off-gas pressure loss

Table 7
Fixed parameters.

	Parameter	Unit	Value
Pumps	Isentropic efficiency	–	0.70
	Motor efficiency	–	0.95
Expander	Isentropic efficiency	–	0.85
	Generator efficiency	–	0.95
Fan	Isentropic efficiency	–	0.90
	Motor efficiency	–	0.95
Heat exchangers	Total heat transfer surface area	(m^2)	750
HRHE	Hydraulic diameter, cold side	(mm)	10
	Hydraulic diameter, hot side	(mm)	60
	Max HRHE off-gas pressure loss	(Pa)	5000
Evaporator	Hydraulic diameter, cold side	(mm)	10
	Hydraulic diameter, hot side	(mm)	20
Condenser	Hydraulic diameter, hot side	(mm)	20
	Hydraulic diameter, cold side	(mm)	20
	Cold side cross-sectional flow area	(cm^2)	100
	Working fluid outlet pressure	(bar)	10
Recuperator	Hydraulic diameter, hot side	(mm)	20
	Hydraulic diameter, cold side	(mm)	10

optimal design of the heat recovery heat exchanger. Instead, we should allow the optimizer to choose the most optimal off-gas pressure loss based on the effect on fan power, as done in Case 2.

In Case 2, half of the fan power from off-gas heat exchanger pressure loss was included during optimization, i.e. $\Delta\dot{W}_{fan,net} = 0.5 \cdot \Delta\dot{W}_{fan,HRHE}$. With this formulation of fan power, the optimizer has an incentive to reduce off-gas pressure loss, yielding a significantly lower pressure loss and fan power than in Case 1. Net power is lower than in Case 1, not only because we have included fan power in the calculation of net power, but also because expander power is lower.

Case 3 accounts for the entire fan power from heat exchanger pressure loss during optimization. This represents the strictest boundary conditions, where a potential reduction in fan power is disregarded. As a result, the optimizer chooses an even lower off-gas pressure loss and equivalent fan power than in Case 2. This case results in the lowest net power, both because of a high net fan power and a low expander power.

Case 1 and Case 3 account for no and all of the fan power from off-gas pressure loss, respectively. In practice, the optimal system solution will lie somewhere between Case 1 and Case 3, depending on the potential for reduction in fan power. We need more knowledge of processes downstream of the system boundary to calculate the exact fan power reduction. However, we can identify two important factors that will impact the fan power reduction. The first is the value of pressure loss through the main processes such as the gas treatment center, wet scrubber and stack. If this pressure loss is high, off-gas cooling has the potential to yield a higher fan power reduction. The other factor is the design of the duct system and the position of the heat recovery heat exchanger in the system; placing this unit close to the electrolysis cells will give a higher potential for pressure loss reduction in the ducts and vice versa. Investigating these factors is an interesting path for future work.

Expander and pumping power differ in Cases 1–3, even though the cases only involve different formulations of fan power from heat exchanger pressure loss. The change in expander and pumping power indicates a coupling between cycle and heat exchanger performance. Table 9 shows the optimized process and heat recovery heat exchanger parameters, which demonstrate the connection between heat exchanger and process parameters. For example, off-gas pressure loss, overall heat transfer coefficient and heat duty in the HRHE decrease from Case 1 to 3, while the surface area and minimum temperature difference increase. At the same time, expander inlet enthalpy and pressure decrease, explaining the reduction in expander power. Since working fluid outlet pressure from the condenser is fixed, a lower expander inlet pressure is coupled to a smaller pressure lift in the working fluid pump and therefore lowers the pumping power. Since these parameters are all the result of a complex overall system optimization, it is difficult to identify a direct link between the different parameters. However, it is obvious that there is a connection between heat exchanger and cycle performance, and that optimum heat exchanger and cycle design both depend on plant-specific factors outside the system boundary.

As mentioned, the surface area of the heat recovery heat exchanger increases from Case 1 to Case 3. This is likely caused by the reduction in off-gas pressure loss and overall heat transfer coefficient, which can be observed in Table 9. Observe also that the HRHE length decreases from Case 1 to Case 3, even though the surface area increases. This is because the optimizer instead chooses to increase cross-sectional flow areas, which more than doubles on the off-gas side from Case 1 to Case 3. This indicates that optimizing only heat exchanger length would not provide a sufficient degree of heat exchanger design freedom.

The cross-sectional flow area on the hot side of the heat recovery heat exchanger is between 100 and 200 times larger than the flow area on the cold side. This is a relatively high ratio, but could be possible in novel heat exchanger concepts for smelter off-gas heat recovery [45].

Table 10 shows the optimized evaporator, condenser and recuperator parameters. Observe that the heat transfer surface areas of these heat exchangers decrease from Case 1 to Case 3, which is coupled to the increasing area requirement of the heat recovery heat exchanger and a fixed total area. Note also that the optimized recuperator length is above zero, implying that recuperation resulted in higher net power.

Since several process and geometry parameters were optimized simultaneously, there is a possibility that the global optimum solution has not been found. To simplify the optimization problem,

Table 8
Main results from system optimization.

Cases	$\dot{W}_{net}$ (kW)	$\dot{W}_{exp}$ (kW)	$\dot{W}_{pumps}$ (kW)	$\Delta\dot{W}_{fan,net}$ (kW)	$\Delta\dot{W}_{fan,HRHE}$ (kW)	Δp_{HRHE} (Pa)
Case 1	118	147	−29.2	0.00	−71.1	5000
Case 2	99.3	135	−26.8	−8.75	−17.5	1230
Case 3	93.1	129	−25.7	−9.72	−9.72	680

Table 9
Optimized process and heat recovery heat exchanger parameters.

	Unit	Case 1	Case 2	Case 3
Process				
$\dot{m}_{wf}$	(kg/s)	2.0	2.0	2.0
$\dot{m}_{ind}$	(kg/s)	2.8	3.2	3.3
$h_{in,exp}$	(kJ/kg)	740	720	720
$p_{in,exp}$	(bar)	51	47	45
$T_{in,HRHE,cold}$	(°C)	65	64	65
HRHE				
L	(m)	35	22	18
$A_{c,hot}$	(cm^2)	4200	7100	9000
$A_{c,cold}$	(cm^2)	39	50	53
A_{HRHE}	(m^2)	510	560	570
$\dot{Q}$	(kW)	850	850	820
U	(W/m^2K)	120	80	68
Δp_{hot}	(Pa)	5000	1200	680
Δp_{cold}	(kPa)	23	12	9
ΔT_{min}	(°C)	13	16	18

we chose to fix some of the parameters that varied little during preliminary optimizations. These parameters include the working fluid pressure at the condenser outlet ($p_{cond,wf}$) and the heat sink mass flow ($\dot{m}_{sink}$). Table 11 shows the optimized values of $p_{cond,wf}$ and $\dot{m}_{sink}$ resulting from the preliminary optimizations, demonstrating a relatively small variation from Case 1 to Case 3, with average values of 10 bar and 23 kg/s, respectively (which were set as the fixed values). Note that the fixed values deviate slightly from the average values in Table 11, owing to results from two cases that were left out.

During the preliminary optimizations, we also optimized the hydraulic diameter on the off-gas side of the heat recovery heat exchanger ($d_{h,gas}$). Table 12 shows the optimized hydraulic diameters in Case 1–3, and Table 13 shows the change in main system optimization results when adding $d_{h,gas}$, $p_{cond,wf}$ and $\dot{m}_{sink}$ as optimization variables. Table 12 demonstrates an increasing trend in hydraulic diameter from Case 1 to Case 3, but Table 13 shows a small impact on net power (only 0.2%) and other optimization results. In fact, net power is reduced in two out of three cases, indicating reduced probability of finding the global optimum with an excessive number of optimization variables. These observations also indicate that optimizing hydraulic diameters is not critical to heat exchanger performance, and supports the assumption that sufficient heat exchanger optimization flexibility can be achieved by optimizing only the cross-sectional flow-area and heat exchanger length.

4. Conclusions

We have optimized Rankine cycle and heat exchangers for power production from aluminum smelter off-gas. The objective was to investigate the effect of fan power on optimum system performance. We developed three cases that accounted for the reduction in fan power by including different parts of the fan power caused by heat exchanger pressure loss. In this way, we could evaluate different conditions in the downstream gas collection and treatment system.

Even though each case was optimized with the same constraint on total heat exchanger surface area, they resulted in significantly different cycle and heat exchanger performance. When fan power was neglected during system optimization, off-gas pressure loss reached the upper limit and fan power became unfeasibly high. However, a high off-gas pressure loss resulted in an efficient heat recovery heat exchanger and a high expander power. On the other hand, when we accounted for the entire fan power from heat exchanger pressure loss, optimization resulted in a relatively low off-gas pressure loss and equivalent fan power. This restricted the performance of the heat recovery heat exchanger and resulted in a relatively low expander power. In practice, the optimum solution depends on the exact value of fan power reduction, which is governed by the total off-gas pressure loss outside the system boundary. Thus, the optimal system solution is unknown, but lies somewhere in the range between the two extremities that account for either none or all of the fan power from heat exchanger pressure loss.

Our analysis also shows that the optimum heat recovery heat exchanger design varies considerably in the different cases, implying that the optimum design depends on the potential for downstream fan power reduction. For example, if the heat recovery heat exchanger is placed close to the electrolysis cells, the potential for pressure loss reduction in the ducts is higher and the heat recovery heat exchanger can be designed with a higher pressure loss. The results also show that there is a strong connection between heat exchanger and cycle performance. Thus, downstream conditions strongly impact both heat exchanger and cycle performance, and should be accounted for during system design. An interesting

Table 10
Optimized evaporator, condenser and recuperator parameters.

	Unit	Case 1	Case 2	Case 3
Evaporator				
L	(m)	77	68	65
$A_{c,hot}$	(cm^2)	28	27	27
$A_{c,cold}$	(cm^2)	39	35	33
A_{evap}	(m^2)	81	65	59
$\dot{Q}$	(kW)	850	850	820
U	(W/m^2K)	2300	2700	2900
Δp_{hot}	(kPa)	40	48	47
Δp_{cold}	(kPa)	86	88	89
ΔT_{min}	(°C)	0.7	1.1	1.1
Condenser				
L	(m)	48	48	43
$A_{c,hot}$	(cm^2)	150	120	120
$A_{c,cold}$	(cm^2)	100	100	100
A_{cond}	(m^2)	120	110	98
$\dot{Q}$	(kW)	720	730	700
U	(W/m^2K)	1300	1400	1400
Δp_{hot}	(kPa)	17	24	24
Δp_{cold}	(kPa)	140	140	130
ΔT_{min}	(°C)	2.4	2.6	3.0
Recuperator				
L	(m)	16	11	11
$A_{c,hot}$	(cm^2)	180	150	150
$A_{c,cold}$	(cm^2)	27	25	23
A_{rec}	(m^2)	38	22	22
$\dot{Q}$	(kW)	110	84	79
U	(W/m^2K)	460	520	520
Δp_{hot}	(kPa)	4.3	3.8	3.9
Δp_{cold}	(kPa)	17	13	15
ΔT_{min}	(°C)	3.0	4.7	4.2

Table 11
Optimized condenser working fluid outlet pressure and heat sink mass flow resulting from preliminary optimizations.

Cases	$p_{cond,wf}$ (bar)	$\dot{m}_{sink}$ (kg/s)
Case 1	10.5	21.9
Case 2	10.4	22.7
Case 3	10.5	22.4
Fixed value	**10**	**23**

Table 12
Optimized hydraulic diameter on off-gas side of the heat recovery heat exchanger resulting from preliminary optimizations.

Cases	$d_{h,gas}$ (mm)
Case 1	55.9
Case 2	60.7
Case 3	66.7
Fixed value	**60**

Table 13
Change in system optimization result when adding condenser working fluid outlet pressure, heat sink mass flow and off-gas side hydraulic diameter as optimization variables.

Cases	$\dot{W}_{net}$	$\dot{W}_{exp}$	$\dot{W}_{pumps}$	$\Delta\dot{W}_{fan,net}$	$\Delta\dot{W}_{fan,HRHE}$	Δp_{HRHE}
Case 1	−0.2%	−1.1%	−4.7%	0.0%	0.0%	0.0%
Case 2	0.2%	−0.6%	−4.0%	0.5%	1.1%	1.6%
Case 3	−0.2%	−1.4%	−5.8%	−1.3%	−1.3%	−1.5%

path for future work is to consider the effect of plant-specific off-gas handling conditions on system performance.

Credit author statement

Monika Nikolaisen: Conceptualization, Methodology, Software, Investigation, Writing - original draft, Writing - review & editing, Visualization, Project administration Trond Andresen: Conceptualization, Methodology, Validation, Writing - review & editing, Visualization, Supervision, Project administration, Funding acquisition

Declaration of competing interest

The authors declare the following financial interests/personal relationships which may be considered as potential competing interests: The authors are employed by the research institute SINTEF Energy Research, wherein their work has been funded by the HighEFF and COPRO projects, which target improvement of industrial energy efficiency.

Acknowledgements

This publication has been funded by the research projects HighEFF and COPRO. HighEFF is a Center for an Energy Efficient and Competitive Industry for the Future, a 8-year Research Center under the FME-scheme (Center for Environment-friendly Energy Research, grant no. 257632/E20). COPRO was a four-year competence building project within industrial surplus-heat-to-power conversion (EnergiX grant no. 255016/E20). The authors gratefully acknowledge the financial support from The Research Council of Norway and user partners of HighEFF and COPRO.

The authors acknowledge Nancy Eik-Nes, Stian Trædal and Brede Hagen for their inputs on language and presentation of the results.

References

[1] Cascella F, Gaboury S, Sorin M, Teyssedou A. Proof of concept to recover thermal wastes from aluminum electrolysis cells using Stirling engines. Energy Convers Manag 2018;172:497–506.
[2] Cullen JM, Allwood JM. Mapping the global flow of aluminum: from liquid aluminum to end-use goods. Environ Sci Technol 2013;47(7):3057–64.
[3] Milford RL, Allwood JM, Cullen JM. Assessing the potential of yield improvements, through process scrap reduction, for energy and CO2 abatement in the steel and aluminium sectors. Resour Conserv Recycl 2011;55(12):1185–95.
[4] Produksjon og forbruk av energi. *energibalanse*. [Accessed 2020-01-28]; Available from: https://www.ssb.no/energi-og-industri/statistikker/energibalanse.
[5] Nowicki C, Gosselin L. An overview of opportunities for waste heat recovery and thermal integration in the primary aluminum industry. JOM 2012;64(8):990–6.
[6] Ladam Y, Solheim A, Segatz M, Lorentsen O-A. Heat recovery from aluminium reduction cells. Light Met 2011:393–8. 2011.
[7] Yu M, Gudjonsdottir MS, Valdimarsson P, Saevarsdottir G. Waste heat recovery from aluminum production. In: Minerals, metals and materials series; 2018. p. 165–78.
[8] Yang F, Zhang H, Yu Z, Wang E, Meng F, Liu H, Wang J. Parametric optimization and heat transfer analysis of a dual loop ORC (organic Rankine cycle) system for CNG engine waste heat recovery. Energy 2017;118:753–75.
[9] Guillaume L, Lemort V. Comparison of different ORC typologies for heavy-duty trucks by means of a thermo-economic optimization. Energy 2019;182:706–28.
[10] Usman M, Imran M, Yang Y, Lee DH, Park BS. Thermo-economic comparison of air-cooled and cooling tower based Organic Rankine Cycle (ORC) with R245fa and R1233zde as candidate working fluids for different geographical climate conditions. Energy 2017;123:353–66.
[11] Mohammadzadeh Bina S, Jalilinasrabady S, Fujii H. Energy, economic and environmental (3E) aspects of internal heat exchanger for ORC geothermal power plants. Energy 2017;140:1096–106.
[12] Orosz MS, Mueller A, Quolin S, Hemond H. Small Scale Solar ORC system for distributed power. SolarPaces 2009.
[13] Pantano F, Capata R. Expander selection for an on board ORC energy recovery system. Energy 2017;141:1084–96.
[14] Song P, Wei M, Zhang Y, Sun L, Emhardt S, Zhuge W. The impact of a bilateral symmetric discharge structure on the performance of a scroll expander for ORC power generation system. Energy 2018;158:458–70.
[15] Declaye S, Quoilin S, Guillaume L, Lemort V. Experimental study on an open-drive scroll expander integrated into an ORC (Organic Rankine Cycle) system with R245fa as working fluid. Energy 2013;55:173–83.
[16] Manente G, Lazzaretto A, Bonamico E. Design guidelines for the choice between single and dual pressure layouts in organic Rankine cycle (ORC) systems. Energy 2017;123:413–31.
[17] Rohde D, Hagen BAL, Trædal S, Andresen T. Comparison of rankine cycle and trilateral flash cycle for power production from low temperature heat sources. Refrigeration Science and Technology 2018.
[18] Braimakis K, Karellas S. Integrated thermoeconomic optimization of standard and regenerative ORC for different heat source types and capacities. Energy 2017;121:570–98.
[19] Elsido C, Mian A, Martelli E. A systematic methodology for the techno-economic optimization of Organic Rankine Cycles. Energy Procedia 2017;129:26–33.
[20] Barzi YM, Assadi M, Parham K. A waste heat recovery system development and analysis using ORC for the energy efficiency improvement in aluminium electrolysis cells. Int J Energy Res 2018;42(4):1511–23.
[21] Barzi YM, Assadi M. Heat transfer and thermal balance analysis of an aluminum electrolysis cell side lines: a heat recovery capability and feasibility study. In: ASME international mechanical engineering congress and exposition, proceedings (IMECE); 2013.
[22] Zhao R, Nowicki C, Gosselin L, Duchesne C. Energy and exergy inventory in aluminum smelter from a thermal integration point-of-view. Int J Energy Res 2016;40(10):1321–38.
[23] Sørhuus A, Wedde G. Pot gas heat recovery and emission control. In: Light metals. Cham: Springer; 2016. B. G., D. M., and T. G., Editors.
[24] Qassab HAA, Mohd SSAA, Wedde G, Sørhuus A. HEX retrofit enables smelter capacity expansion. In: Suarez CE, editor. Light metals 2012. Cham: Springer International Publishing; 2016. p. 815–20.
[25] de Gromard A, Lim C, Bouhabila EH, Cloutier B, Frainais M. Development on electrolytic cell gas cooling. In: Grandfield J, editor. Light metals 2014. Cham: Springer International Publishing; 2016. p. 623–8.
[26] Sørhuus AK, Ose S, Nilsen BM. Possible use of 25 MW thermal energy recovered from the potgas at alba line 4. In: Hyland M, editor. Light metals 2015. Cham: Springer International Publishing; 2016. p. 631–6.
[27] Nowicki C, Gosselin L, Duchesne C. Waste heat integration potential assessment through exergy analysis in an aluminum production facility. Energy Technology. In: Carbon dioxide management and other technologies. Hoboken, NJ, USA: John Wiley & Sons Inc; 2012. 2012.
[28] Fleer M. Heat recovery from the exhaust gas of aluminum reduction cells. Iceland: Reykjavík University; 2010.
[29] Castelli AF, Elsido C, Scaccabarozzi R, Nord LO, Martelli E. Optimization of organic rankine cycles for waste heat recovery from aluminum production plants. Frontiers in Energy Research 2019;7(44).
[30] Wang Z, Zhou N, Luo L, Guo J. Thermodynamic analysis of power generation system based on waste heat from aluminium reduction cell. Light Metals; 2010.
[31] Ladam Y, Børgund M, Næss E. Influence of heat source cooling limitation on ORC system layout and working fluid selection: the case og aluminium industry. In: TMS light metals; 2014.
[32] Børgund MA. Power production from low temperature aluminium electrolysis cell off-gases. In: Department of energy and process engineering. Norwegian University of Science and Technology; 2009.
[33] Kolasiński P. In: The application of ORC systems for waste heat recovery in metal smelting industry; 2019. ORC2019.
[34] Bouhabila EH, Næss E, Einejord VK, Kristjansson K. An innovative compact heat exchanger solution for aluminum off-gas cooling and heat recovery. In: Sadler BA, editor. Light metals 2013. Cham: Springer International Publishing; 2016. p. 793–7.
[35] Sorhuus A, Rye K, Nyland G. Increased energy efficiency and reduced HF emission with new heat exchanger. Light metals. 2010. p. 249–54.
[36] Hagen BAL, Nikolaisen M, Andresen T. *A novel methodology for Rankine cycle analysis with generic heat exchanger models* Applied Thermal Engineering. 2020.
[37] Solheim A, Senanu S. Recycling of the flue gas from aluminium electrolysis cells. In: Light metals 2020. Cham: Springer International Publishing; 2020.
[38] Aarhaug TA, Ratvik AP. Aluminium primary production off-gas composition and emissions: an overview. JOM 2019;71(9):2966–77.
[39] Lemmon EW, Huber ML, McLinden MO. NIST standard reference database 23: reference fluid thermodynamic and transport properties-REFPROP. 2013. Version 9.1.
[40] Gnielinski V. New equations for heat and mass transfer in turbulent pipe and channel flow, vol. 16; 1976. p. 359–68. April.
[41] Selander WN. Explicit formulas for the computation of friction factors in turbulent pipe flow. Chalk River, Ontario, Canada: Chalk River Nuclear Labs; 1978.
[42] Boyko LD, Kruzhilin GN. Heat transfer and hydraulic resistance during condensation of steam in a horizontal tube and in a bundle of tubes. Int J Heat Mass Tran 1967;10(3):361–73.
[43] Friedel L. Improved friction pressure drop correlations for horizontal and

vertical two-phase pipe flow, vol. 18; 1979. p. 485–91.
[44] Schittkowski K. NLPQL: a fortran subroutine solving constrained nonlinear programming problems. Ann Oper Res 1986;5(1):485–500.
[45] Skjervold VT, Skaugen G, Andresen T, Nekså P. Enabling power production from challenging industrial off-gas – model-based investigation of a novel heat recovery concept. In: IIR international rankine 2020 conference -heating. Glasgow, UK: Cooling and Power Generation; 2020.